

## Phonon characterization of $\text{YBa}_2(\text{Cu}_{1-x}\text{Al}_x)_3\text{O}_{7-\delta}$ by Raman spectroscopy

P. B. Kirby, M. R. Harrison, W. G. Freeman, I. Samuel, and M. J. Haines

*GEC Research Limited, Hirst Research Centre, East Lane, Wembley, Middlesex HA9 7PP, United Kingdom*

(Received 28 August 1987; revised manuscript received 13 October 1987)

We present new Raman scattering data on high-temperature superconducting materials with composition  $\text{YBa}_2(\text{Cu}_{1-x}\text{Al}_x)_3\text{O}_{7-\delta}$ . In  $\text{YBa}_2\text{Cu}_3\text{O}_{7-\delta}$  we observe new high-frequency peaks greater than  $700\text{ cm}^{-1}$  that we associate with two-phonon interactions of the first-order Cu—O Raman vibrations that occur at 337,  $(450 \pm 10)$ , and  $502\text{ cm}^{-1}$ . The intensity of these new peaks suggests that anomalous phonon interactions are taking place. Results on Al substitution are consistent with a unit-cell change from orthorhombic to tetragonal. The observation of superconductivity in the tetragonal structure means that it is not possible to simply assign superconductivity to the orthorhombic structure.

There have been several reports on Raman scattering from the recently discovered high-temperature superconductors.<sup>1-4</sup> The interest in applying Raman spectroscopy to these materials is two-fold. First, it might provide information on the mechanism of superconductivity by either measurements of the superconducting energy gap or by identification of a strong electron-phonon interaction.<sup>5</sup> Second, it should provide a means of characterizing what has so far been a multiphase material. The latter aim has already been realized by Rosen *et al.*,<sup>1</sup> who have convincingly demonstrated the superiority of Raman over x-ray analysis for locating the presence of different phases. Such identification is important before detailed conclusions can be made. Batlogg *et al.*<sup>6</sup> have studied phonon shifts by Raman spectroscopy upon isotope substitution and have taken the invariance of the superconducting transition temperature as evidence that a strong electron-phonon interaction is not present in these materials. However, comparison with the work of Rosen<sup>1</sup> suggests that two of Batlogg *et al.* peaks ( $592$  and  $644\text{ cm}^{-1}$ ) can be associated with the presence of a  $\text{BaCuO}_2$  phase. Stavola *et al.*<sup>2</sup> have argued that the  $500(\pm 5)\text{ cm}^{-1}$  peak arises from the bridging O atoms, it being the Cu—O atoms perpendicular to the *c* axis that are crucial for the superconducting behavior. As an aid to phonon identification we have accumulated the identification of all Raman peaks observed to date in Table I. It is clear that great care must be taken in identifying modes in the superconducting phase.

The samples of  $\text{YBa}_2(\text{Cu}_{1-x}\text{Al}_x)_3\text{O}_{7-\delta}$  were prepared by firing suitable amounts of  $\text{Y}_2\text{O}_3$ ,  $\text{BaCO}_3$ ,  $\text{CuO}$ , and  $\text{Al}_2\text{O}_3$  (British Drug Houses Analar grade). These were mixed in an agate mortar with a pestle for 15 min and then pressed into rectangular bars ( $2.5 \times 5 \times 2.5\text{ mm}^3$ ). The bars were then placed in alumina boats and fired in a tube furnace at  $950^\circ\text{C}$  for 60 h in flowing oxygen. After this period, the furnace was turned off and the bars left to cool to below  $200^\circ\text{C}$  over a period of 6 h. They were then removed from the furnace.

Portions of the samples were examined by x-ray powder diffraction to determine the phases present. Samples not containing any Al ( $x=0.00$ ) showed only diffraction peaks corresponding to the orthorhombic form of

$\text{YBa}_2\text{Cu}_3\text{O}_{7-\delta}$  ( $\delta \leq 0.5$ ). In contrast, the samples where 5% of the Cu ions in the starting mixture was replaced by Al ions ( $x=0.05$ ) showed only peaks corresponding to the tetragonal form of  $\text{YBa}_2\text{Cu}_3\text{O}_{7-\delta}$  ( $\delta > 0.5$ ). Thus a transition from orthorhombic to tetragonal symmetry occurs at an intermediate composition. Samples containing higher concentrations of Al ions contained other phases besides the tetragonal form of  $\text{YBa}_2\text{Cu}_3\text{O}_{7-\delta}$ ; these phases were identified as  $\text{BaAl}_2\text{O}_4$  and  $\text{Y}_2\text{BaCuO}_5$ .

Resistance measurements were made on bars cut from the samples using the normal four-probe method with contacts attached to the bars using silver paint. A current of 10 mA was used corresponding to an approximate current density of  $0.05\text{ mA cm}^{-2}$  and Fig. 1 shows the results obtained. The resistivity of the sample not containing any aluminum ( $x=0.00$ ) shows a sharp drop at 92 K but does not reach "zero" resistance until 88 K. The normal-state resistivity of the  $x=0.05$  sample is very similar but the superconducting transition is much broader and the zero resistance state is not achieved until 82 K. The normal-state resistivity increases with increasing Al content and the superconducting transition broadens still further.

Raman spectra were taken with a Spex 1404 monochromator having holographic gratings. Resolution was generally better than  $5\text{ cm}^{-1}$ . Photon counting techniques were used with scan times up to 24 h. The excitation source was the  $5145\text{-\AA}$  line of an argon-ion laser. For the low-temperature measurements the material was mounted in vacuum which eliminated atmospheric scattering. As much care must be taken in recording the spectra as in identifying modes. The material was found to degrade under moderate laser intensities and so the incident intensities used here were less than 40 mW, though greater intensities were possible at low temperature. No attempt is made here to identify the laser-damaged parts, but it seems possible that such irradiation could prove useful for converting to nonsuperconducting regions in small devices. It is believed that the results presented here are characteristic of the as-received material. It was found, however, that the surface region of a sample often gave unrepresentative spectra and so it was common practice in this work to remove the surface layer by gentle grinding

TABLE I. Reported Raman peaks to date in different phases of YBaCuO. The first number refers to the Raman peak in  $\text{cm}^{-1}$ , the second refers to the phase identified in the original paper:  $O_s$  for  $\text{Y}_2\text{BaCuO}_5$ ,  $O_2$  for  $\text{BaCuO}_2$ ,  $O_{so}$  for the orthorhombic superconducting state and,  $O_{st}$  for the tetragonal state. The third number refers to the relative intensity found by the original authors for that peak amongst the member peaks of a certain phase.

Rosen <i>et al.</i> (Ref. 1)	Hemley and Mao (Ref. 1)	Stavola <i>et al.</i> (Ref. 2)	Macfarlane, Rosen, and Siki (Ref. 3)	Batlogg <i>et al.</i> (Ref. 4)
	106, $O_s$ ,8			
	142, $O_s$		153, $O_s$	
187, $O_s$ ,3	180, $O_s$ ,13			
204, $O_s$ ,4	204, $O_s$ ,9			
220, $O_2$ ,4	222, $O_s$ ,12			
241, $O_s$ ,8	233, $O_s$ ,14			
267, $O_s$ ,9	265, $O_s$ ,11			
293, $O_s$ ,6	292, $O_s$ ,11			
319, $O_s$ ,3	317, $O_s$ ,3			
337, $O_s$ ,2	338, $O_s$ ,2		337, $O_s$	
(388, $O_s$ )	389, $O_s$ ,2			
391, $O_s$ ,2				
427, $O_2$ ,3				
441, $O_s$ ,11	(450, $O_s$ )	435, $O_{so}$	441, $O_s$	433, $O_s$ ,4
473, $O_s$ ,7	447, $O_s$ ,6	470, $O_{st}$		
	483, $O_s$ ,1	495, $O_{so}$		
502, $O_s$ ,1			502, $O_s$ ,1	501, $O_s$ ,2
	517, $O_s$ ,10			
563, $O_s$ ,10	560, $O_s$ ,5			
587, $O_2$ ,2		590, $O_t$		592, $O_s$ ,3
605, $O_s$ ,1	603, $O_s$ ,1		601, $O_s$	
		625, $O_t$		
635, $O_2$ ,1				644, $O_s$ ,1

on course glasspaper followed by the fine glasspaper. Excess particles were then brushed off with a clean cotton swab. Attempts were made to produce polished samples but flatness to 10 wavelength fringes was always accompanied by pits of missing material.

First of all we compare our Raman spectra to recently published data. Figure 2(a) shows a typical Raman spectrum recorded on our superconductor sample. Table II lists the peaks we have observed on a single sample at

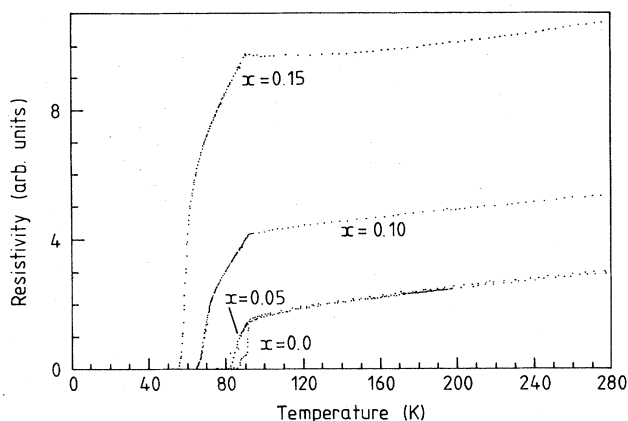


FIG. 1. Resistance measurements vs temperature for different aluminum substitutions in  $\text{YBa}_2(\text{Cu}_{1-x}\text{Al}_x)_3\text{O}_{7-\delta}$ .

various positions (including depths). An extreme example of an atypical spectrum is shown in Fig. 2(b). Typically in the range  $300\text{--}700\text{ cm}^{-1}$  the spectrum is dominated by the Raman peaks at  $336$  and  $502\text{ cm}^{-1}$ , the latter being the most intense. The additional peaks seen in Fig. 1(b) can be seen by reference to Table I to be due to the presence of the  $\text{BaCuO}_2$  phase (Ref. 1).

A group theory analysis of orthorhombic  $\text{YBa}_2\text{Cu}_3\text{O}_{7-\delta}$ , which has space group  $D_{2h}$  leads to the conclusion that there are three Raman active modes that involve oxygen displacements.<sup>2</sup> These correspond to the  $A_g$ ,  $B_{2g}$ , and  $B_{3g}$  representations. By comparison with the Raman spectrum of  $\text{Cu}_2\text{O}$ ,<sup>7</sup> it has been taken that the  $\text{Cu}\text{--O}$  vibrations occur near  $500\text{ cm}^{-1}$ . It has been suggested that two modes  $B_{2g}$  and  $B_{3g}$  should be degenerate due to the similar  $\text{Cu}\text{--O}$  bond lengths.<sup>2,4</sup> Indeed Liu *et al.* have made a tentative assignment of modes in the  $400\text{--}650\text{ cm}^{-1}$  frequency range. However, comparison with Table I suggests that their assignment of the  $E_g$  mode (with their  $432\text{ cm}^{-1}$  peak) and two disorder activated transitions (with their  $584$  and  $640\text{ cm}^{-1}$  peaks) are due to the presence of  $\text{BaCuO}_2$ . The consistency of our results, and the evidence of others, suggest that the  $502$ ,  $337$ , and  $440(\pm 10)\text{ cm}^{-1}$  Raman peaks are the modes characteristic of the superconducting orthorhombic phase.

Additional evidence for this association comes from the observation here, for the first time, of phonon modes at frequencies greater than  $700\text{ cm}^{-1}$ . Examples of these occur in Figs. 2(a), 3(a), and 4(a)–4(c). Structure of this sort is always observed at room temperature consisting

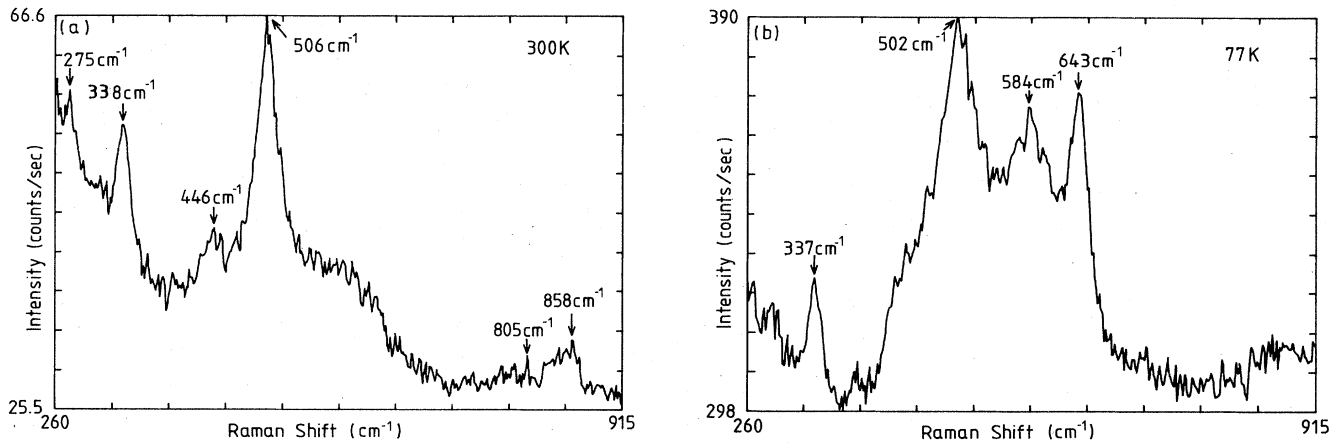


FIG. 2. (a) Most typical Raman spectrum obtained at 300 K on our superconductor. In the range 300–700  $\text{cm}^{-1}$  the peaks at 337 ( $443 \pm 10$ ), 502  $\text{cm}^{-1}$  are always seen. (b) Extreme example of Raman spectrum. The additional peaks are due to the presence of the  $\text{BaCuO}_2$  phase. (Arrows on figures indicate a position on the abscissa, not necessarily a peak position.)

very often of well-defined peaks at ( $786 \pm 20$ )  $\text{cm}^{-1}$  and ( $856 \pm 10$ )  $\text{cm}^{-1}$ . The sharpest linewidth observed for the 856  $\text{cm}^{-1}$  peak is 25  $\text{cm}^{-1}$ , comparable to the peaks at lower frequencies. The lower-energy peak ( $786 \pm 20$ )  $\text{cm}^{-1}$  is not always well resolved, showing more variability than that at 856  $\text{cm}^{-1}$  (see Table II).

We suggest that two-phonon interactions are being observed at high frequencies, the strong intensities indicating that such interactions are particularly strong in  $\text{YBa}_2\text{Cu}_3\text{O}_{7-\delta}$ . It is of interest that anomalously large two-phonon interactions have been observed in materials where there are  $d$ -electrons at the Fermi level,<sup>8</sup> a situation thought to prevail in  $\text{YBa}_2\text{Cu}_3\text{O}_{7-\delta}$ . These peaks are worthy of further study. The frequency shifts observed for these peaks are consistent with them being the result

of combinations of (i) the 337 and 443  $\text{cm}^{-1}$  peaks to give the 786  $\text{cm}^{-1}$  peak [in Fig. 2(a)] and (ii) the 337 and 502  $\text{cm}^{-1}$  peaks to give the 840- $\text{cm}^{-1}$  peak. Such an association can only be made if the additive phonons come from a single phase. Generally, overtone processes, i.e., the sum of a mode at wave vector  $\mathbf{k}$  and the same mode at  $-\mathbf{k}$ , provide the strongest features in the two-phonon Raman spectra of perfect crystals. Without matrix-element enhancement the Raman spectrum should resemble the phonon density of states when the frequency scales are adjusted by a factor of 2. Combination and difference processes in a perfect crystal involve different modes at  $\mathbf{k}$  and  $-\mathbf{k}$  and usually produce weaker spectra. Two-phonon processes are not restricted to  $k=0$  phonons and contributions usually occur across all the Brillouin zone, and so it

TABLE II. Raman peaks observed in this study on a single sample at various positions. A column of numbers refers to the Raman peaks observed in a given position, the Raman frequency is given in  $\text{cm}^{-1}$ . All spectra were recorded at 300 K except columns 7 and 10 (from the left) that were measured at 77 K.

300 K	300 K	300 K	300 K	300 K	300 K	77 K	300 K	300 K	77 K
				140		148	147	139	146.5
				164			176	176	164
				209		213			
				231					
		275							
	294								
337.5	337	337	337.5	342	337.5	336	337	337	341.5
						(388)			
443	465	440	446	451	454	446		457.5	448
504	502	503	507	504	505	502	502	502	504
	518								
				586	586		571	579	580
				650	643		636		636
786		803		801	Broad smear				
						no peaks			no peaks
856		856		860			860	860	

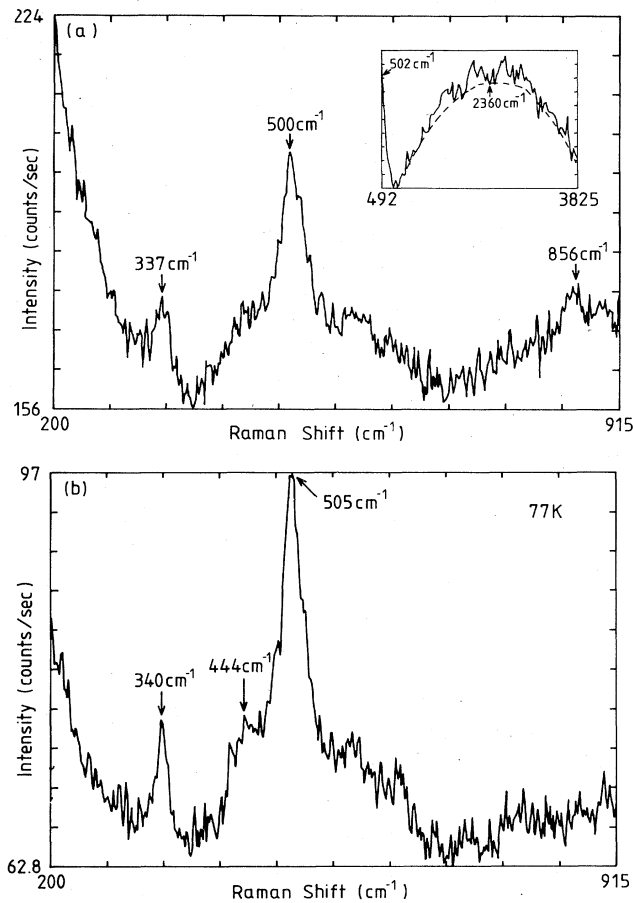


FIG. 3. (a) Room-temperature Raman spectra from orthorhombic  $\text{YBa}_2(\text{Cu}_{1-x}\text{Al}_x)_3\text{O}_{7-\delta}$ . The inset shows the high-energy response using 488-nm excitation. (b) Raman spectrum recorded at the same position as (a) but at 77 K.

is surprising therefore that the second-order peaks are so narrow.

In Figs. 3(a) and 3(b) we present spectra recorded from the same position on the sample at 300 and 77 K. The rising background signal below  $300\text{ cm}^{-1}$  is due to parasitic scattering of laser light. There is little change in the character of the peaks in the  $300\text{--}700\text{ cm}^{-1}$  range except perhaps a small reduction in peak linewidths which enables clearer identification of peaks on the low-frequency shoulder of the  $502\text{ cm}^{-1}$  peak. A more definitive study of the low-frequency modes ( $<300\text{ cm}^{-1}$ ) is the basis for further study. The only noticeable change on going to 77 K is the considerable reduction in the intensity of the assigned second-order spectrum. At 300 K the ratio of the recorded signal at  $502\text{ cm}^{-1}$  to that at  $857\text{ cm}^{-1}$  is 0.87, whereas at 77 K it is 0.68, this latter value being a lower bound due to the background count signal at  $856\text{ cm}^{-1}$ . This background is larger at low temperature because of the extra parasitic scattering due to the presence of our cryostat. This is typical of two-phonon processes that generally fade away quickly with decreasing temperature. Further studies will be important for an assessment of the

electron-phonon contribution to the high-temperature superconducting transition. A unique aspect of the scattering in the high-temperature superconductor is revealed in the inset of Fig. 3(a) with scattering taking place at very large Raman shifts. This extremely broad structure has not, to our knowledge, been seen in any other material system in nature, being  $2000\text{ cm}^{-1}$  wide and peaked at  $\sim 2400\text{ cm}^{-1}$  (0.3 eV). We found that excitation energy dependences are consistent with a scattering process. Our preliminary results indicate little temperature dependence of the form of the spectrum. It is tempting to associate this feature with a broad feature observed in infrared reflectivity measurements at 0.37 eV that was associated with excitation across an energy gap.<sup>9</sup> Whatever the final explanation, it is clear that this scattering process provides a direct, experimentally manipulable manifestation of the electronic excitations which appear to mediate superconductivity in this material. Raman measurements on single crystals are needed to investigate this scattering process.

We now turn to our Raman spectra obtained on materials where Al is substituted for Cu in the starting materials

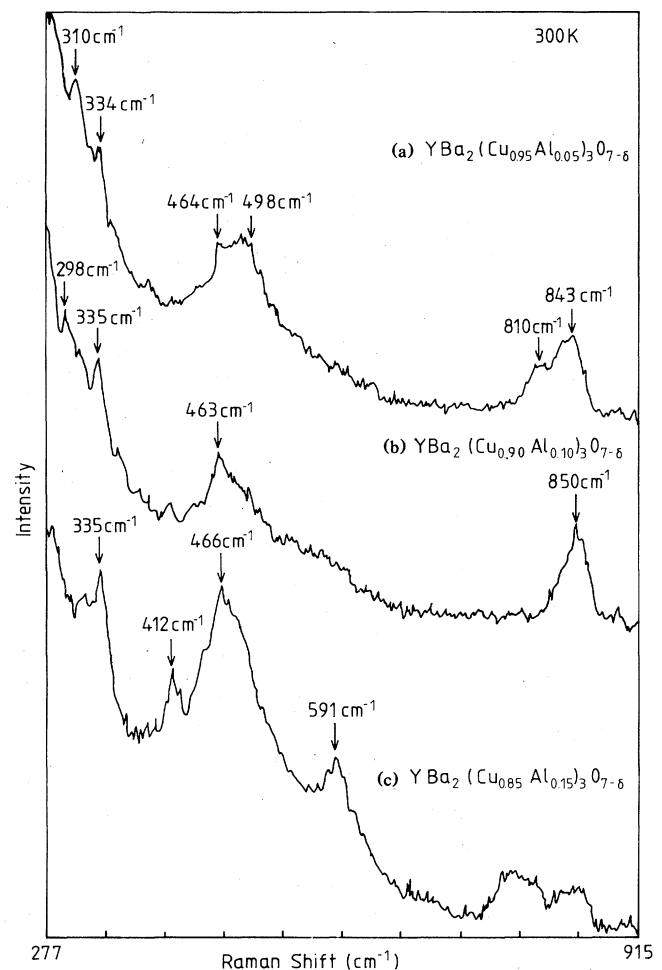


FIG. 4. (a) Raman spectrum of 5% Al substituted sample. (b) Raman spectrum of 10% Al substituted sample. (c) Raman spectrum of 15% Al substituted sample.

used for preparation of  $\text{YBa}_2\text{Cu}_3\text{O}_{7-\delta}$ . The recorded spectra for 5% and 10% aluminum content are displayed in Figs. 4(a) and 4(b) and reveal large changes in the first-order spectra with new peaks appearing. We concentrate again on the 300–700  $\text{cm}^{-1}$  region. It is seen that the 502  $\text{cm}^{-1}$  peak first of all broadens, developing a flat top shape [Fig. 4(a)], and then, with increasing Al content becomes peaked at 464  $\text{cm}^{-1}$ . This behavior is very similar to that reported by Stavola *et al.*<sup>2</sup> who studied the changing Raman spectra upon annealing orthorhombic  $\text{YBa}_2\text{Cu}_3\text{O}_{7-\delta}$  in argon when the oxygen content changed from  $\text{O}_{6.95}$  through to  $\text{O}_{6.01}$ . It is now established that over this range the material changes from the orthorhombic ( $\delta \leq 0.5$ ) to tetragonal ( $\delta \geq 0.5$ ). The tetragonal structure was found to be nonsuperconducting. The difference between the two structures is now thought to be the absence of oxygen atoms in the direction to the O–Cu–O (i.e., perpendicular to the so-called superconducting ribbons). The main change observed by Stavola *et al.*<sup>2</sup> was a shift in their main 495  $\text{cm}^{-1}$  phonon peak to 470  $\text{cm}^{-1}$  when annealing was complete. This change was argued by these authors to be associated with the Ag symmetric stretching motion of the oxygen atoms bridging the CuO planes. The change in frequency of this mode was accounted for by the fact that the *c* axis is longer in the tetragonal unit cell. It is common for the frequency to go as the inverse of the bond length to the fourth power. It has already been noted that x-ray analysis reveals that the 5% Al substituted sample is tetragonal.

Our results on aluminum substituted samples can be explained in a similar way. We have already noted that x-ray analysis revealed that our 5% Al substituted samples was tetragonal. For this sample no new Raman peaks were observed in the 300–700  $\text{cm}^{-1}$  frequency range meaning that any new phases make up a very small percentage of the sample. However, the 15% Al substituted Raman spectrum [Fig. 4(c)] shows evidence of a

$\text{Y}_2\text{BaCuO}_5$  phase from the observation of a peak at 590  $\text{cm}^{-1}$  (see Table I). Additional Raman peaks seen for this sample cannot be associated with previous phases identified by Raman spectroscopy<sup>1</sup> and so are perhaps consistent with the suggestion from x-ray analysis that  $\text{BaAl}_2\text{O}_4$  is present.

From the fact that superconductivity was not observed in the annealed tetragonal sample Stavola *et al.*<sup>2</sup> concluded that the linear Cu–O chains are critical for superconductivity. Our results complicate this picture since the change to a tetragonal structure upon Al substitution occurs without the loss of the superconducting behavior. Further techniques are required to fully characterize these samples. However, it appears that Al can replace Cu in  $\text{YBa}_2\text{Cu}_3\text{O}_{7-\delta}$  to the limited extent of about 5% without producing impurity phases. This is confirmed by our recent resistivity studies with Al < 5%. We note that the shift of the Raman mode at 502 to 464  $\text{cm}^{-1}$  is accompanied by an increase in the linewidth, suggesting that the sublattice containing the Cu–O chains is more disordered. We find no evidence for a broadening of the 336  $\text{cm}^{-1}$  mode perhaps suggesting that this mode is associated with the unaffected Cu–O ribbons between the barium and yttrium atoms.

In conclusion, our Raman studies on  $\text{YBa}_2(\text{Cu}_{1-x}\text{Al}_x)_3\text{O}_{7-\delta}$  show many similarities with the tetragonal phase of  $\text{YBa}_2\text{Cu}_3\text{O}_{7-\delta}$ . More definitive structural studies are necessary to elucidate the interplay between oxygen stoichiometry, Cu–O disorder, and the Cu valence state. Combined structural, electrical, and Raman studies on material with  $x < 0.05$  should provide detailed information on these dependences and their effect on the superconducting transition temperature.

We thank Dr. Karl Gehring for his encouragement of the collaborations necessary to perform this work.

<sup>1</sup>H. Rosen, E. M. Engler, T. C. Strand, V. Y. Lee, and D. Bethune, *Phys. Rev. B* **36**, 726 (1987); R. J. Hemley and H. K. Mao, *Phys. Rev. Lett.* **58**, 2340 (1987).

<sup>2</sup>M. Stravola, D. M. Krol, W. Weber, S. A. Sunshine, A. Jayaraman, G. A. Kourouklis, R. J. Cava, and E. A. Rietman, *Phys. Rev. B* **36**, 850 (1987).

<sup>3</sup>R. M. Macfarlane, H. Rosen, and H. Siki, *Solid State Commun.* **63**, 831 (1987).

<sup>4</sup>R. Liu, R. Merlin, M. Cardona, H. Mattausch, W. Bauhofer, and A. Simon, *Solid State Commun.* **63**, 839 (1987).

<sup>5</sup>R. Sooryakumar and M. V. Klein, *Phys. Rev. Lett.* **45**, 660 (1980).

<sup>6</sup>B. Batlogg, R. J. Cava, A. Jayaraman, R. V. van Dover, G. A. Kourouklis, S. Sunshine, D. W. Murphy, L. W. Rupp, H. S. Chen, A. White, K. T. Short, A. M. Muzsca, and E. A. Rietman, *Phys. Rev. Lett.* **58**, 2333 (1987).

<sup>7</sup>A. Compaan and H. Z. Cummins, *Phys. Rev. B* **6**, 4753 (1972).

<sup>8</sup>H. Wipf, M. V. Klein, and W. S. Williams, *Phys. Status Solidi (b)* **108**, 489 (1981).

<sup>9</sup>K. Kamarás, C. D. Porter, M. G. Doss, S. L. Herr, D. B. Tanner, D. A. Bonn, J. E. Greedan, A. H. O'Reilly, C. V. Stager, and T. Timusk, *Phys. Rev. Lett.* **59**, 919 (1987).